Desalination and Water Treatment
www.deswater.com
doi: 10.1080/19443994.2014.903525

54 (2015) 2777–2793
May

Taylor & Francis
Taylor & Francis Group

Extended isotherm and kinetics of binary system dye removal using carbon nanotube from wastewater

Niyaz Mohammad Mahmoodi*, Jalil Ghobadi

Department of Environmental Research, Institute for Color Science and Technology, Tehran, Iran, Tel. +98 021 22969771; Fax: +98 021 22947537; email: nm_mahmoodi@icrc.ac.ir

Received 23 October 2013; Accepted 5 March 2014

ABSTRACT

This paper investigates the ability of multi-walled carbon nanotube (CNT) to adsorb three cationic dyes from colored wastewater in single and binary systems. Basic Blue 41 (BB41), Basic Red 18 (BR18), and Basic Violet 16 (BV16) were used as model dyes. The surface characteristic of CNT was studied using Fourier transform infrared. The effect of operational parameters (CNT dosage, dye concentration, pH, and salt) on dye removal was investigated. The adsorption isotherm and kinetic were studied. The isotherm data in single and binary systems followed Langmuir isotherm. The maximum adsorption capacity (Q_0) of BB41, BR18, and BV16 in single dye systems were 123.457, 80.012, and 64.935 mg/g, respectively. In adsorption from binary dye solutions, the isotherm of each individual dye followed extended Langmuir isotherm model. The paper also measured the kinetic adsorption of the dyes on CNT in single and binary dye systems at different dye concentrations. The adsorption follows a pseudo-second-order kinetic model at all the concentrations and values on the rate constants (k_2) in binary systems at optimum dye concentration (25 mg/L) have been calculated as 0.612, 0.548, and 0.517 g/mg min, respectively. Results showed CNT was an effective adsorbent to remove cationic dyes from single and binary systems.

Keywords: Multi-walled carbon nanotube; Binary system; Dye removal; Isotherm; Colored wastewater

1. Introduction

Dyes as an important class of pollutants are often found in the waterways as a result of their wide industrial use. Several industries such as textile consume substantial volume of water and also use dyes to color its products. The exact number (and also the amount) of the dyes produced in the world is not known. It is estimated to be more than 100,000 commercially available dyes. Some of dyes are known to be carcinogenic [1–12].

Dye removal from aqueous phase is a challenge concern as the discharge regulations become more stringent. Thus, there is a need to have a method, which may work suitably and should be cost effective for the dye removal [13–16]. Different methods were used to remove dyes from wastewater such as Fenton oxidation [17], electrochemical treatment [18], photochemical degradation [19,20], etc.

Each method has different color removal capabilities, capital costs and operating rates [21–23].

*Corresponding author.

Adsorption process has been found to be superior to other processes for pollutant removal in terms of cost, simplicity of design, ease of operation, and insensitivity of toxic substances [24–27].

Carbon nanotubes (CNT) are highly popular due to their properties like high thermal, electrical, and mechanical properties. High porosity and layered structure of CNT make it a possible candidate to remove pollutants such as trihalomethanes [28], microcystins [29], fluoride [30], lead [31], nickel [32], and arsenate [33] that are presented in natural water resources [34,35]. The surface of CNT provides distributed hydrophobic sites for pollutants. Different studies suggested that hydrophobic interactions could not generally explain the interactions between organic chemicals and CNT. Other mechanisms include π–π interactions between bulk π systems on CNT surface and organic molecules with C=C double bonds or benzene rings, hydrogen bonds, and electrostatic interactions must be considered, accordingly [36,37].

CNT has different environmental applications. It was used as a photocatalyst to degrade dyes [1], lead (II) removal [38], and chromium removal using magnetic CNTs [39]. Dye removal from single systems (only one dye in solution) using CNT was studied [40,41]. However, a literature review showed that CNT was not used to remove cationic dyes from binary systems (mixture of two dyes in solution) while dye removal ability of other adsorbents such as Activated Carbon [42], Feldspar [43], Alginate [44], Dendrimer [45], etc. have been studied in detail. In this study, CNT was used as an adsorbent to remove cationic dyes (Basic Blue 41 (BB41), Basic Red 18 (BR18), and Basic Violet 16 (BV16)) from single (sin) and binary (bin) systems (Fig. 1). Effective parameters (CNT dosage, dye concentration, pH, and salt), isotherm, and kinetic studies were investigated to evaluate the adsorption capacity of CNT in single and binary systems of dyes. The Langmuir isotherm was used to fit the equilibrium data. Moreover, extended Langmuir

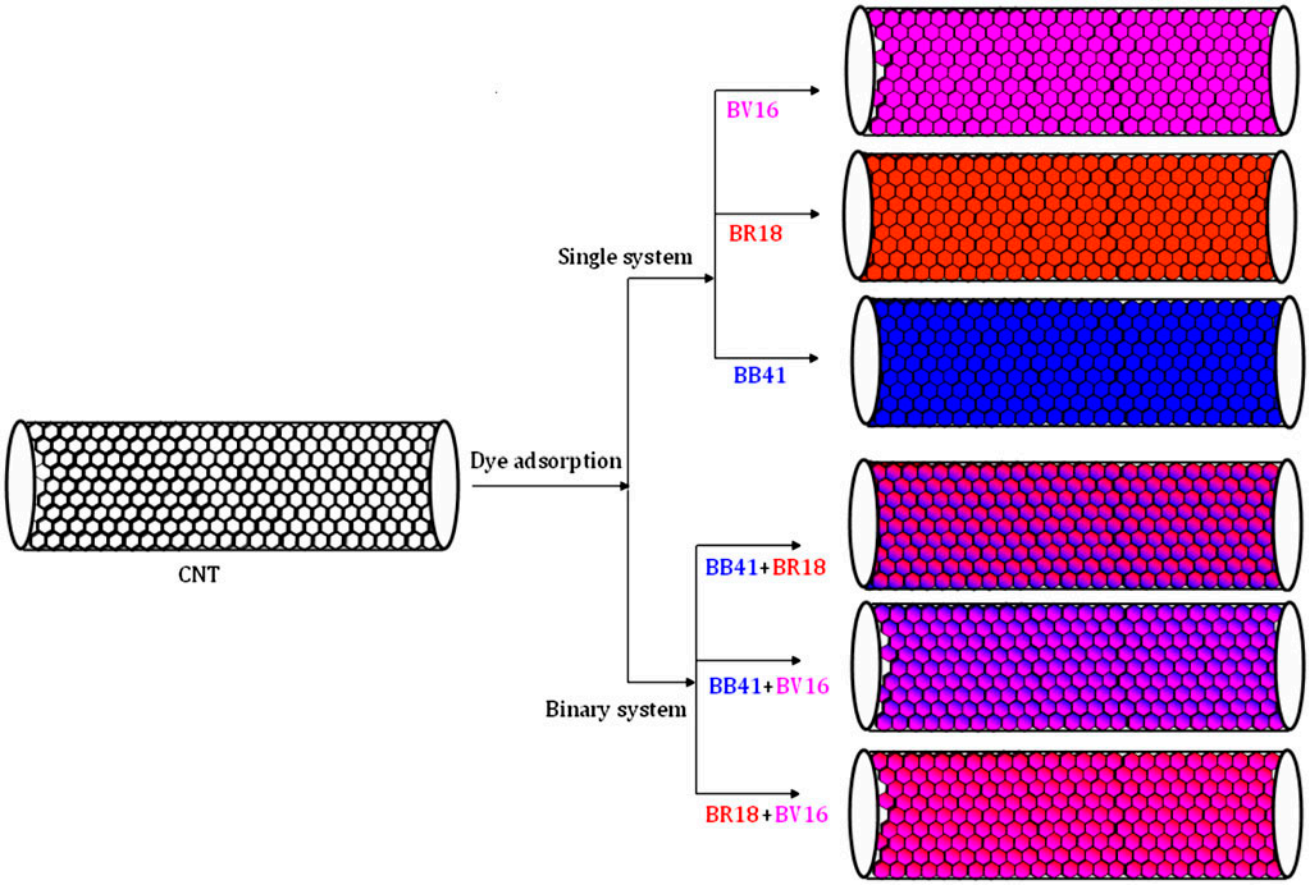

Fig. 1. Dye removal using CNT from single (BB41, BR18, and BV16) and binary systems (BB41 + BR18, BB41 + BV16, and BR18 + BV16).

isotherm was performed to gain further insight into the adsorption process of binary systems. Pseudo-first-order and pseudo-second-order kinetic models were attempted.

2. Experimental

The multi-walled CNT (appearance: black powder, number of walls: 3–15, specific surface area (BET, N_2): 240 m^2/g, outer diameter/inner diameter/length: 5–20 nm/2–6 nm/1–10 μm, purity (Carbon): >95% and apparent density: 150–350 g/cm^3) was purchased from Plasma Chem GmbH (Germany). Basic dyes were BB41, BR18, and BV16. The dyes were obtained from Ciba and used without further purification. The chemical structure of dyes was shown in Fig. 2. All other chemicals were purchased from Merck (Germany).

UV–vis spectrophotometer CECIL 2021 was used for absorbance measurements of samples. The maximum wavelength (λ_{max}) of BB41, BR18, and BV16 to determine residual dye concentration in solution was 605, 488, and 545 nm, respectively. In order to investigate the surface characteristics of CNT, Fourier transform infrared (FTIR) (Perkin–Elmer Spectrophotometer Spectrum One) was studied. For dyes in single systems, the amount of dye adsorbed at equilibrium per unit of mass, q_e, was calculated as follows (Eq. (1)):

$$q_e = (C_0 - C_e)V/m \tag{1}$$

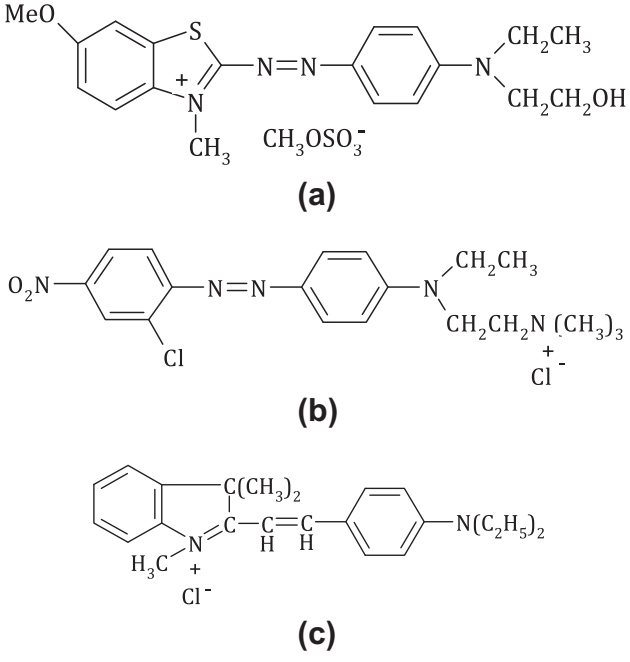

Fig. 2. The chemical structure of dyes (a) BB41, (b) BR18, and (c) BV16.

where C_0 and C_e are the initial and equilibrium concentrations of dye in solution (mmol/L), respectively, V is the volume of dye solution (L), and m is the mass of the adsorbents used (g).

In binary system dye concentrations were calculated as follows: for a binary system of components A and B measured at λ_1 and λ_2, respectively, to give optical densities of d_1 and d_2 (Eqs. (2) and (3)) [25]:

$$C_A = (k_{B_2}d_1 - k_{B_1}d_2)/(k_{A_1}k_{B_2} - k_{A_2}k_{B_1}) \tag{2}$$

$$C_B = (k_{A_1}d_2 - k_{A_2}d_1)/(k_{A_1}k_{B_2} - k_{A_2}k_{B_1}) \tag{3}$$

where k_{A1}, k_{B1}, k_{A2}, and k_{B2} are the calibration constants for components A and B at the two wavelengths λ_1 and λ_2, respectively. The amount of i dye adsorbed at equilibrium per unit of mass, $q_{e,i}$, was calculated as follows (Eq. (4)) [46]:

$$q_{e,i} = (C_{0,i} - C_{e,i})V/m \tag{4}$$

where $C_{0,i}$ and $C_{e,i}$ are the initial and equilibrium concentrations of i dye in the mixture (mmol/L), respectively, V is the volume of dye mixture (L), and m is the mass of the adsorbents used (g).

The percentage of dye adsorption by the adsorbents was computed using Eq. (5):

$$\text{Dye removal}_{(i)} = ((C_{0,i} - C_{e,i})/C_{0,i}) \times 100 \tag{5}$$

where C_0 and C_e represent the initial and equilibrium concentration of dyes (mg/g) in the solutions, respectively. All tests were carried out in duplicate to insure the reproducibility of the results, the mean of the two measurements is reported.

For investigating the effect of operational parameters on the dye removal in single and binary systems by CNT, range of the experimental variables was chosen as follows: adsorbent dosage (0.04–0.12 g), dye concentration (25–100 mg/L), pH values (2–9), and salts (Blank, NaCl, $NaHCO_3$, and Na_2SO_4). Table 1 shows the initial amount of dye concentration which was used in single and binary systems for each dye.

For investigating the effect of adsorbent dosage on removal ability of adsorbents in both single and binary systems, 250 mL of dye solution (25 mg/L) at pH 7.5 were prepared. Different amounts of CNT (0.04–0.12 g) were applied and the mixtures were agitated for 60 min using jar test at room temperature (25°C). In this step, optimum amount of adsorbents for each dye was determined.

For investigating the effect of initial dye concentration on the percentage of dye removal in both single

Table 1
Initial dye concentration used in single and binary systems

Single system (BB41, BR18, BV16) C_0	Binary system (BB41, BR18, BV16) C_0
25	25
50	50
75	75
100	100

and binary systems, 250 mL of dye solutions with different concentrations (25, 50, 75, and 100 mg/L) at pH 7.5 were prepared. The optimum amount of adsorbent in single systems (0.08 g for BB41 and BR18, 0.10 g for BV16) and in binary systems (0.08 g for BB41 + BR18 and BB41 + BV16, 0.10 g for BR18 + BV16) were added to above-mentioned mixtures at room temperature.

The effect of pH on dye removal of single and binary systems were studied by contacting 250 mL of dye solution (25 mg/L) at different pH values (2, 5, 7.5 and 9) and optimum amount of CNT, using jar test at room temperature.

For studying the effect of inorganic ions on the percentage of dye removal of both single and binary systems, 250 mL of dye solution (25 mg/L) at pH 7.5 were prepared and optimum amount of adsorbent for each dye at each system were added. These solutions were agitated in jar test with 0.02 M of different salts (NaCl, $NaHCO_3$, and Na_2SO_4).

At different time intervals, the reaction mixtures were collected, centrifuged, and analyzed for the residual dye concentration using spectrophotometer spectrum one beam, Perkin-Elmer, USA.

3. Results and discussion

3.1. Effect of operational parameters

3.1.1. Effect of adsorbent dosage

A given mass of CNT can adsorb only a fixed amount of dye. Thus, determining the initial dosage of CNT is very important. The effect of CNT dosage on dye removal of BB41, BR18, and BV16 in single and binary systems by varying the amounts of CNT in the range of 0.04–0.12 g was considered. The experiments was carried out by contacting 250 mL of dye solution with initial dye concentration of 25 mg/L using jar test at a fixed pH of 7.5, and room temperature (25˚C) for 60 min. The dye removal results are represented in Fig. 3.

Based on Fig. 3, the percentage of dye removal increased with increasing of the CNT dosage up to a certain amount and then it reached to a constant value. The increase in dye adsorption with adsorbent dosage is due to the increase of adsorbent surface and availability of more adsorption sites. However, if the adsorption capacity was expressed in mg/g of material, the capacity decreased with the increase in the amount of adsorbent. It can be attributed to overlapping or aggregation of adsorption sites resulting in a decrease in total adsorbent surface area available to the dye and an increase in diffusion path length [9].

3.1.2. Dye concentration effect

The effects of dye concentration in single and binary systems of dyes on the percentage of dye removal were studied. Optimum amounts of CNT was added to 250 mL of single and binary systems, at different dye concentrations of 25, 50, 75, and 100 mg/L at a fixed pH (7.5).

For single and binary systems, the equilibrium capacity decreased with an increase in the initial dye concentration as shown in Fig. 4. In the case of lower dye concentrations, the ratio of initial number of dye moles to the available adsorption sites is low. At higher concentrations, the number of available adsorption sites became lower and subsequently, the removal of dyes depends on the initial dye concentration. At the high concentrations, it is not likely that dyes only adsorb in a monolayer at the outer interface of adsorbent [9,47,48].

3.1.3. Effect of initial pH

The influence of pH on removal efficiency of basic dyes was assessed to gain further insight into the adsorption process. The experiments were carried out at jars containing 250 mL of dye solutions with 25 mg/L initial concentration and optimum dosage of adsorbent. Fig. 5 shows dye removal ability of CNT as a function of time at different pH values. The optimum pH for both single and binary dye removal systems was determined to be 7.5.

The results showed that dye adsorption increased when pH increased from 2 to 7.5, and also adsorption of dyes did not significantly alter beyond 7.5. It means that the charge sign on surface of the CNT should be negative in a wide pH range. Thus, cationic dye adsorption onto CNT increased with increase in the pH values suggested that one of the contributions of CNT adsorption toward cationic dyes resulted from electrostatic attraction between the negatively charged CNT adsorbent surface and the positively charged cationic dyes [40].

3.1.4. Inorganic salts effect

The inorganic anions exist in dye-containing industrial wastewater [1–3]. These substances may compete

for the active sites on the adsorbent surface or deactivate the adsorbent and subsequently, decrease the dye adsorption efficiency. A major drawback resulting from the non-selectivity of adsorbent is that it also reacts with non-target compounds present in the background water matrix, i.e. dye auxiliaries present in the

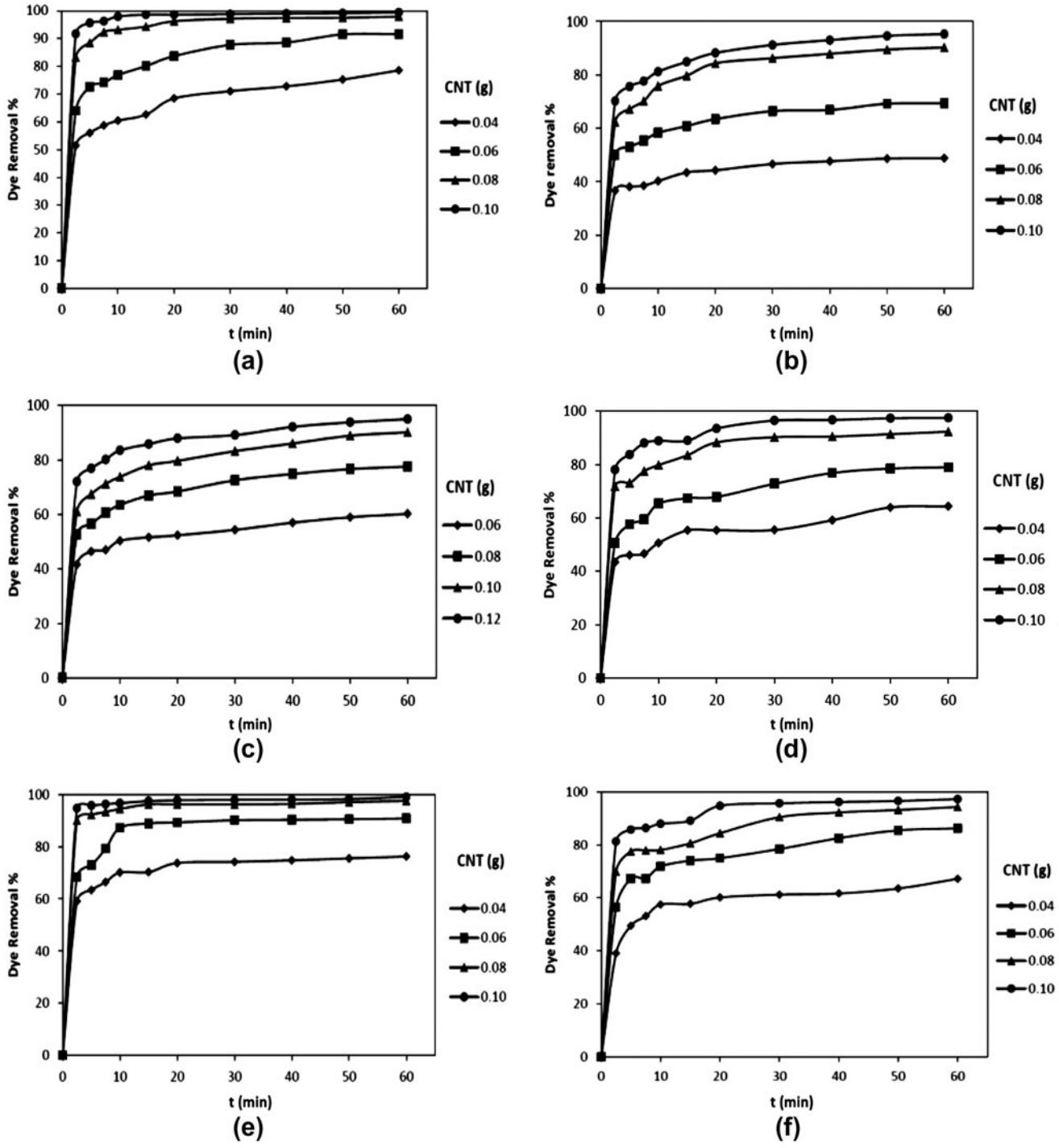

Fig. 3. Effect of adsorbent dosage (g) on dye removal by CNT (initial concentration: 25 mg/L, pH: 7.5, temperature: 25˚C) (a) BB41 (sin), (b) BR18 (sin), (c) BV16 (sin), (d) BB41 (bin, BB41 + BR18), (e) BB41 (bin, BB41 + BV16), (f) BR18 (bin, BB41 + BR18), (g) BR18 (bin, BR18 + BV16), (h) BV16 (bin, BB41 + BV16), (k) BV16 (bin, BR18 + BV16).

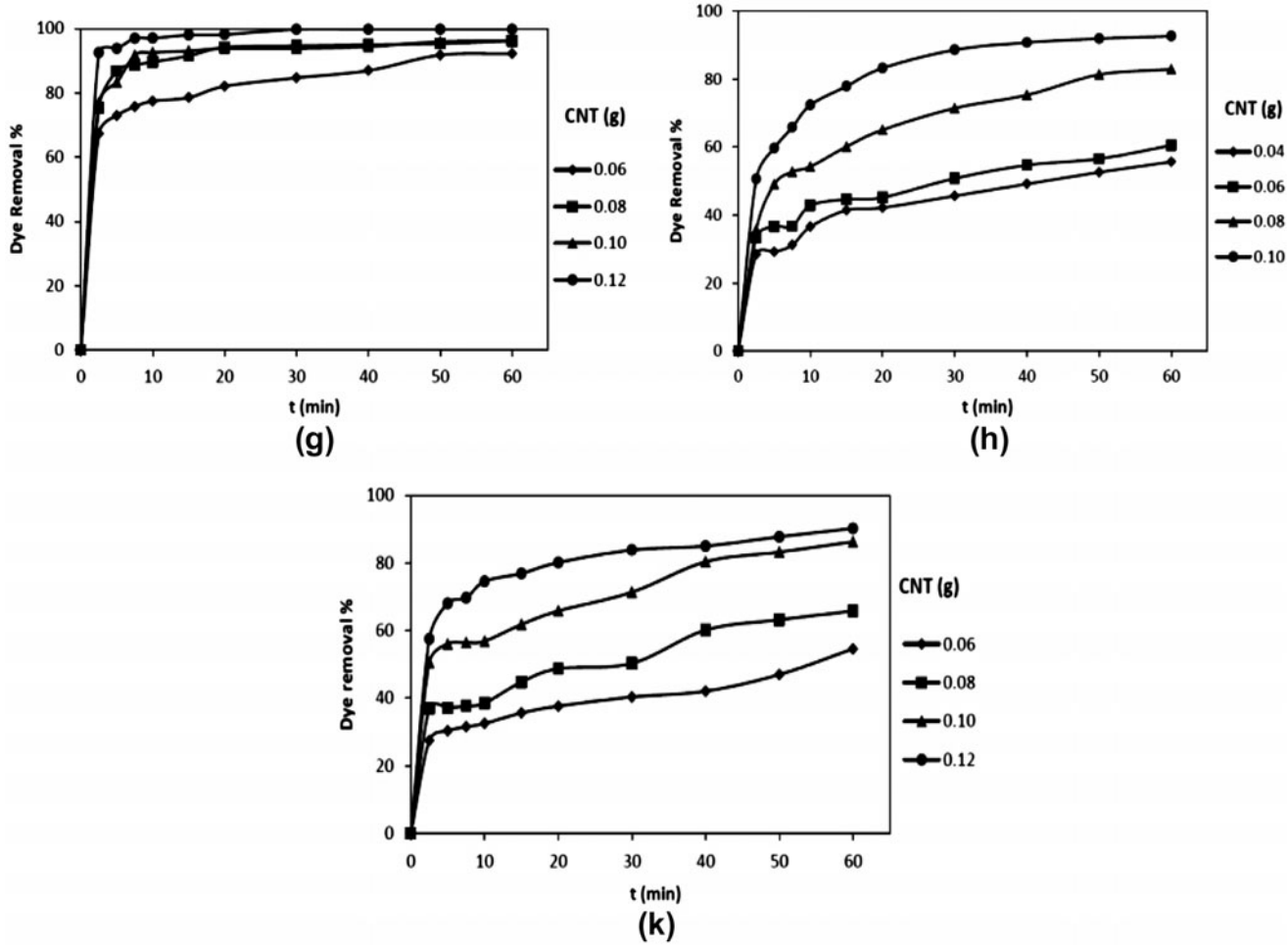

Fig. 3. (*Continued*).

exhausted dye bath. It results higher adsorbent dosage demand to accomplish the desired degree of dye removal efficiency.

The influence of inorganic salts on dye removal ability of CNT in both single and binary systems were studied by adding 0.02 M of NaCl, $NaHCO_3$, and Na_2SO_4 into 250 mL dye solution of 25 mg/L initial concentration, optimum amount of adsorbent dosage, and at constant pH value of 7.5. The results indicate that dye removal capacity of CNT is decreased in single and binary systems in the presence of inorganic salts (Figures not shown). It can be attributed that these salts are small molecules and they can compete with dye molecules in adsorption by CNT.

3.2. Adsorption isotherm models in single and binary dye solutions

In order to design an effective adsorption system to remove dyes from solutions, it is important to establish the most appropriate correlation for the equilibrium curve. Many models have been used in literatures to describe the experimental data of adsorption isotherms. The Langmuir model is the most frequently employed model and given by (Eq. (6)) [49]:

$$q_e = Q_0 K_L C_e/(1 + K_L C_e) \quad (6)$$

where q_e, C_e, Q_0, and K_L are the amount of dye adsorbed at equilibrium (mg/g), the concentration of adsorbate at equilibrium (mg/L), maximum adsorption capacity(mg/g), and Langmuir constant (L/mg), respectively. The linear form of Eq. (6) is represented as follows (Eq. (7)):

$$C_e/q_e = 1/K_L Q_0 + C_e/Q_0 \quad (7)$$

To study the applicability of the Langmuir isotherm for dye adsorption onto the CNT surface in

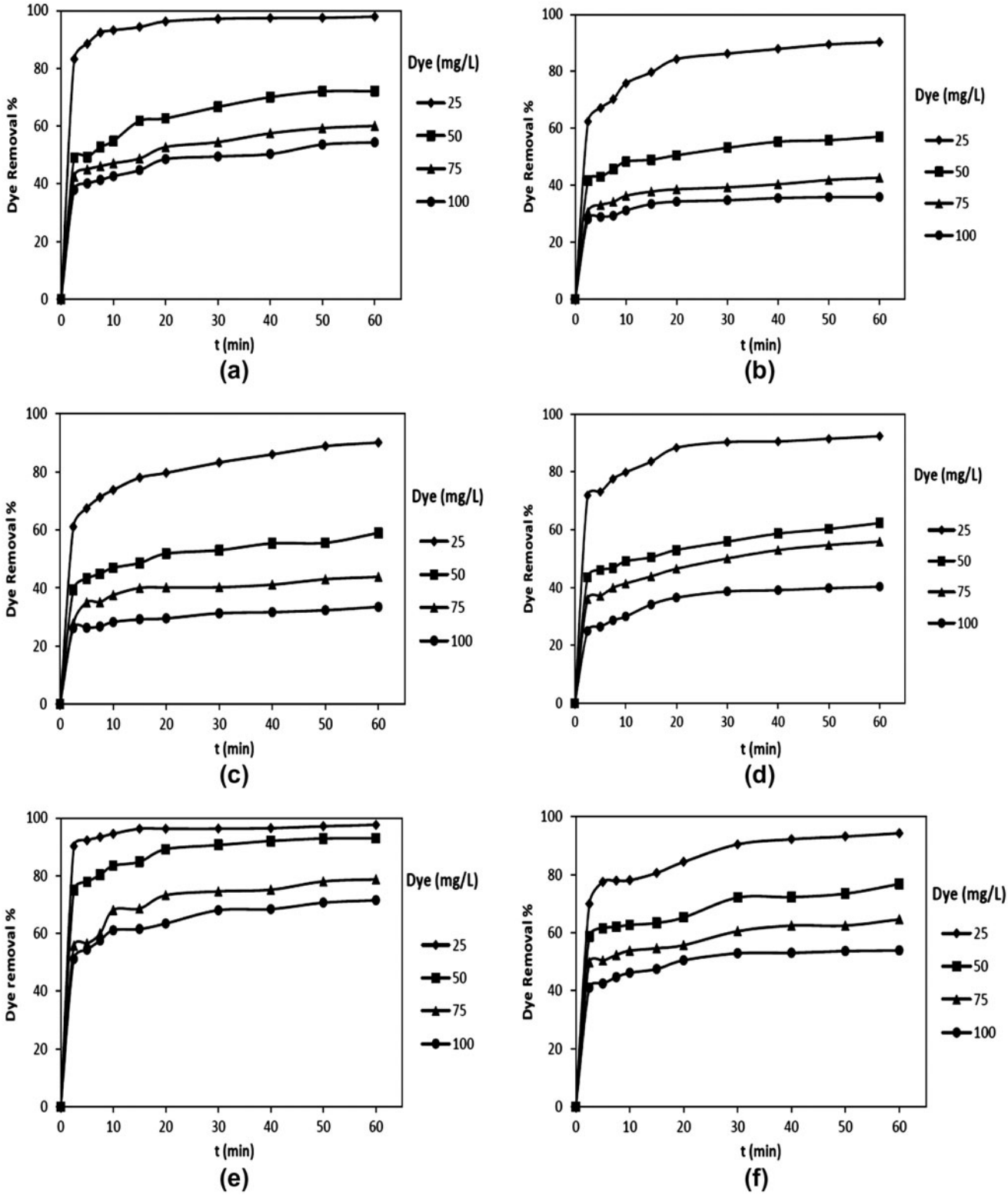

Fig. 4. Effect of dye concentration (mg/L) on dye removal by CNT (adsorbent dosage: optimum amounts, pH: 7.5, temperature: 25˚C) (a) BB41 (sin), (b) BR18 (sin), (c) BV16 (sin), (d) BB41 (bin, BB41 + BR18), (e) BB41 (bin, BB41 + BV16), (f) BR18 (bin, BB41 + BR18), (g) BR18 (bin, BR18 + BV16), (h) BV16 (bin, BB41 + BV16), (k) BV16 (bin, BR18 + BV16).

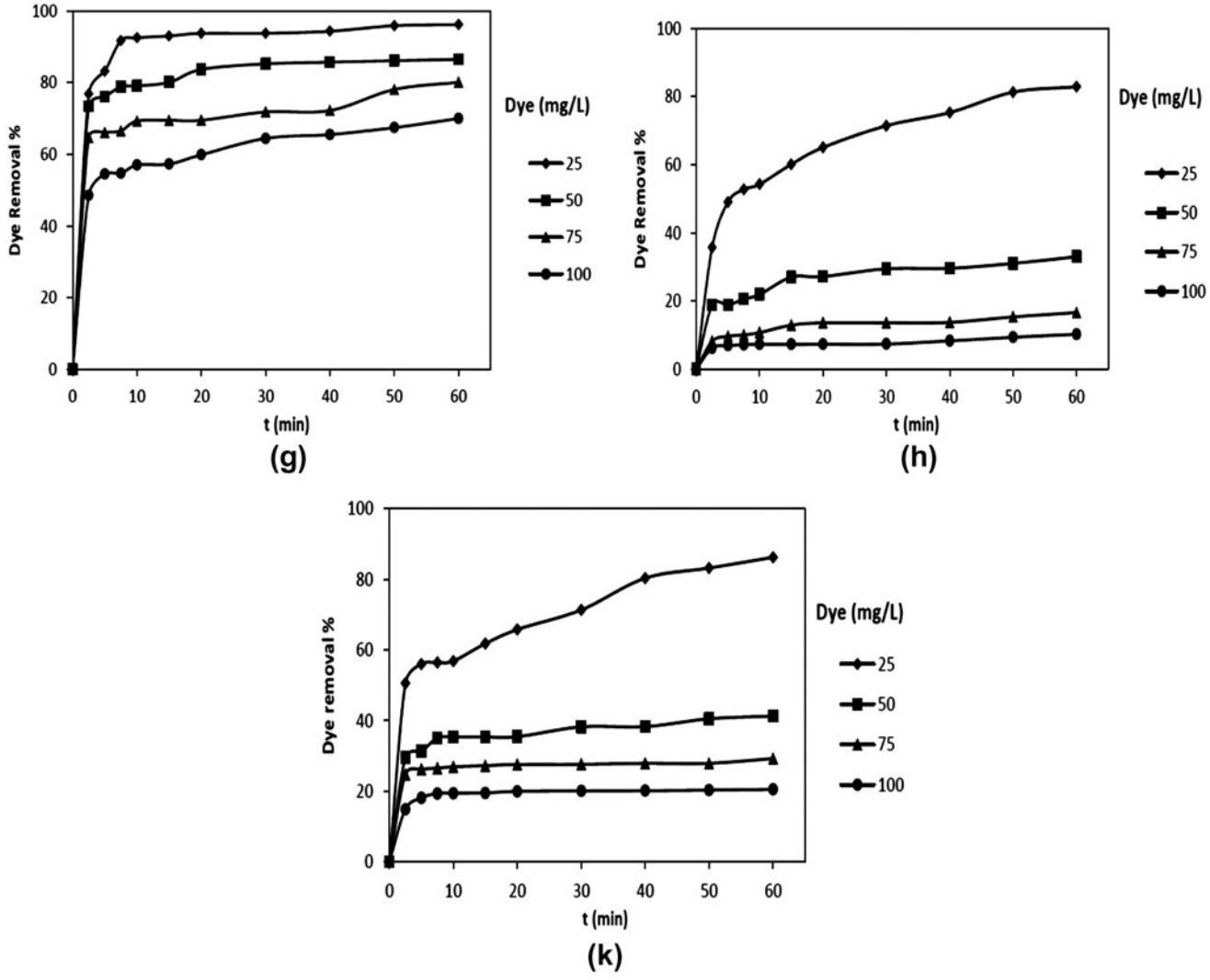

Fig. 4. (*Continued*).

single systems, linear plot of C_e/q_e against C_e is plotted. The values of Q_0, $K_{L,}$ and R^2 are shown in Table 3.

The linear fit between the C_e/q_e vs. C_e and calculated correlation coefficients (R^2) in single dye solutions show that the dye removal isotherm can be approximated as Langmuir model ($R^2 = 0.99$). This means that the adsorption of dyes takes place at specific homogeneous sites and a one layer adsorption onto CNT surface occurs [50].

Moreover, the maximum adsorption capacities for individual dyes in single dye mixtures are shown in Table 2. A good correlation could be established between Q_0 and chemical structure of the dyes. The adsorption capacity of BB41 is higher than that of BR18 and BV16. This is explained on the basis of higher molecular weight of BB41 (482 g/mol) comparing to BV16 and BR18 (367 g/mol and 426 g/mol, respectively). Two main mechanisms that play an important role in adsorption of these basic dyes onto the surface of the CNTs are electrostatic and hydrophobic interactions [1]. Because of the higher molecular weight of BB41 there is a strong affinity between hydrophobic moieties of BB41 and CNTs by π-π stacking [51]. Furthermore, hydrogen bonds may form between tube surfaces of OH and the OH substitution on the BB41 and also OH substitution enhance π-π interactions between the dye molecule and CNTs [52].

Moreover, a comparison is made between the maximum adsorption capacities of different adsorbents for a specific dye (Basic Blue 9). From Table 2 it is obvious that CNT has an appropriate adsorption capacity in comparison with other adsorbents [53–59].

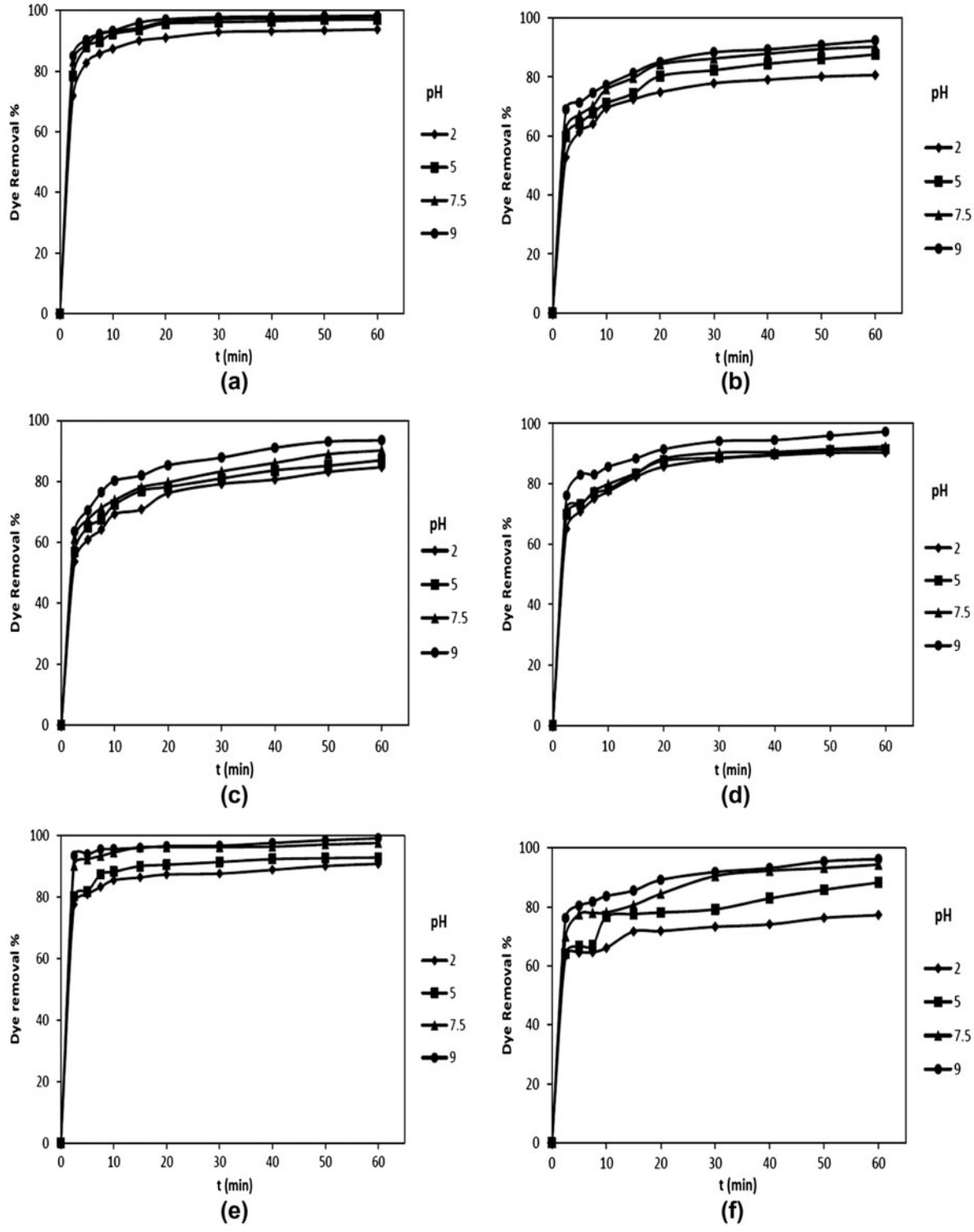

Fig. 5. Effect of pH on dye removal by CNT (adsorbent dosage: optimum amounts, initial concentration: 25 mg/L, temperature: 25˚C), (a) BB41 (sin), (b) BR18 (sin), (c) BV16 (sin), (d) BB41 (bin, BB41 + BR18), (e) BB41 (bin, BB41 + BV16), (f) BR18 (bin, BB41 + BR18), (g) BR18 (bin, BR18 + BV16), (h) BV16 (bin, BB41 + BV16) and (k) BV16 (bin, BR18 + BV16).

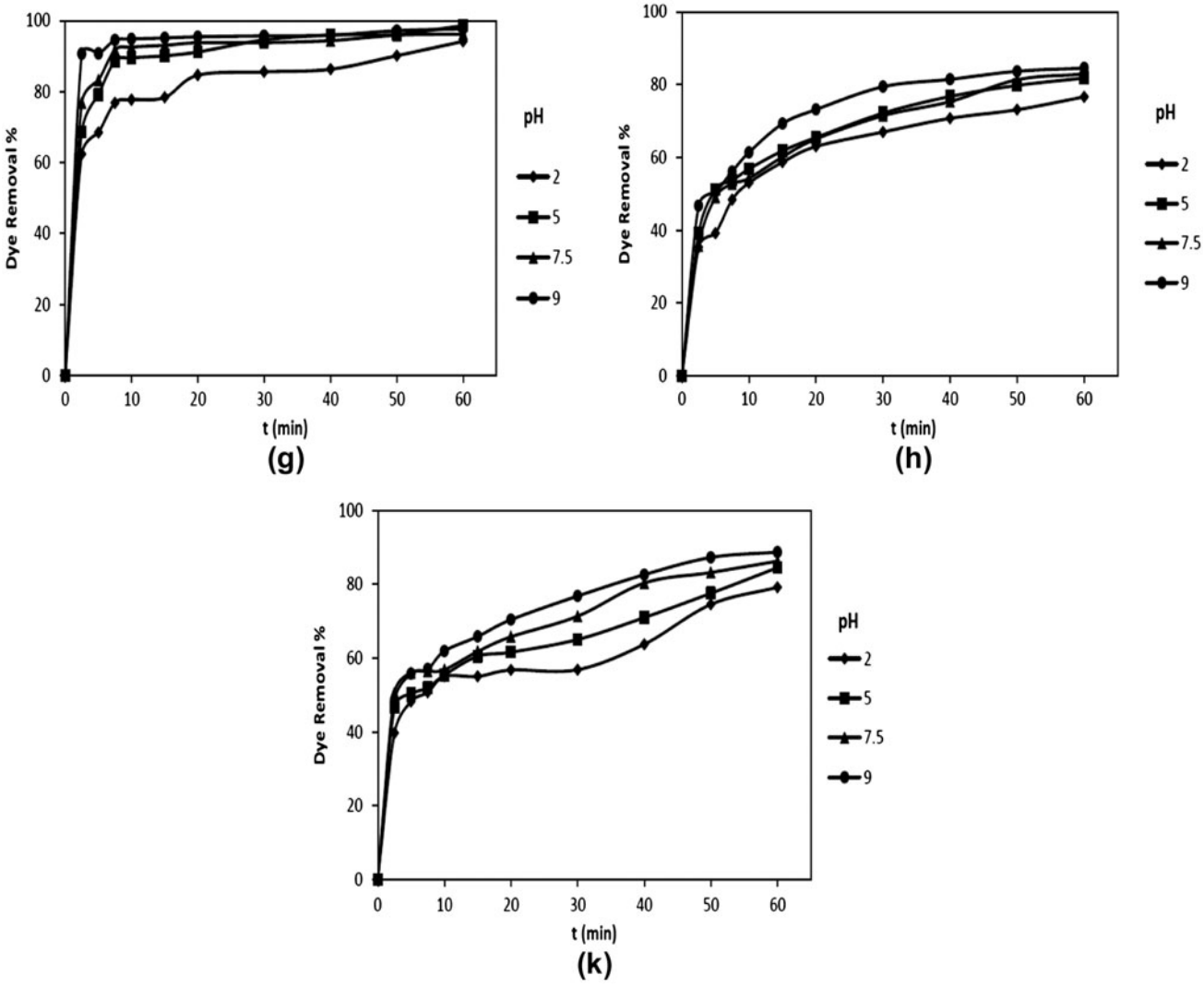

Fig. 5. (*Continued*).

As previously discussed, the adsorption isotherms of the three dyes were followed the Langmuir type in single dye mixtures, while the isotherm of an each dye in binary dye solutions had less regular shape than normal Langmuir isotherm model. In this study, an extended Langmuir model was applied to fit the experimental data.

Extended Langmuir isotherm model is the most general used model in multi-component systems, which permitted derived from the basis of single-component Langmuir model (Eq. (7)). The extended Langmuir is presented by the Eq. (8) [60]:

$$q_{e,i} = Q_{0,i}K_{L,i}C_{e,i}/(1 + \sum K_{L,i}C_{e,i}) \quad (8)$$

where $K_{L,i}$ is the adsorption equilibrium constant of dye i in mixed dye system.

In dye adsorption from binary solutions, the quantities of dye adsorbed were expressed as (Eqs. (9) and (10)) [61]:

$$q_{e,1} = Q_{0,1}K_{L,1}C_{e,1}/(1 + K_{L,1}C_{e,1} + K_{L,2}C_{e,2}) \quad (9)$$

$$q_{e,2} = Q_{0,2}K_{L,2}C_{e,2}/(1 + K_{L,1}C_{e,1} + K_{L,2}C_{e,2}) \quad (10)$$

According to Eqs. (9) and (10), we have (Eq. (11)):

$$K_{L,2}C_{e,2}/K_{L,1}C_{e,1} = Q_{0,1}q_{e,2}/Q_{0,2}q_{e,1} \quad (11)$$

Table 2
Adsorption capacities of different adsorbents for removal of cationic dyes

Adsorbent	Dye	Q_0 (mg/g)	Ref.
Cotton waste	Basic Blue 9	277	[53]
Coal	Basic Blue 9	250	[53]
Rice husk	Basic Blue 9	312	[53]
Hair	Basic Blue 9	158	[53]
Sewage sludge	Basic Blue 9	115	[54]
Groundnut shell carbon	Basic Blue 9	165	[55]
Raw date pits	Basic Blue 9	80	[56]
Clay	Basic Blue 9	300	[57]
Diatomite	Basic Blue 9	198	[58]
Carbonaceous adsorbent	Basic Blue 9	92	[59]
Bamboo dust carbon	Basic Blue 9	143	[55]
MWCNTs	Basic Red 18	80	Present study
MWCNTs	Basic Blue 41	123	Present study
MWCNTs	Basic Violet 16	65	Present study

After rearrangement, a linear form of the extended Langmuir isotherm in binary dye system was obtained (Eq. (12)) [62]:

$$C_{e,1}/q_{e,1} = 1/K_{L,1}Q_{0,1} + C_{e,1}/Q_{0,1} + q_{e,2}C_{e,1}/q_{e,1}Q_{0,2} \quad (12)$$

According to Eq. (12), the values of $C_{e,1}/q_{e,1}$ had linear correlation with $C_{e,1}$ and $C_{e,1}q_{e,2}/q_{e,1}Q_{0,2}$ if the adsorption obeyed the extended Langmuir model. By using Eq. (12) as the fitting model, the isotherm parameters of an individual dye in the binary dye solutions were predicted (Table 3). From Table 3, it is obvious that the isotherms of an individual dye in the binary dye systems followed the extended Langmuir model which their correlation coefficients (R^2) were in the range of 0.988–0.999.

The extended Langmuir isotherm is based on the same basic assumptions as those for the single-component Langmuir isotherm. Therefore, if interaction and competition occurs, the extended Langmuir isotherm will not be suitable for representing this system [62].

Table 3
Langmuir isotherm constants for BB41, BR18, and BV16 in single and binary dye solutions

Dye		Q_0	K_L	R^2
Langmuir				
Single	BB41	123.457	2.613	0.990
	BR18	80.012	1.984	0.995
	BV16	64.935	2.484	0.999
Extended Langmuir				
BB41 + BR18	BB41	116.412	2.354	0.994
	BR18	71.225	1.857	0.990
BB41 + BV16	BB41	107.117	2.097	0.989
	BV16	63.004	2.226	0.995
BR18 + BV16	BR18	68.854	1.553	0.988
	BV16	55.057	1.993	0.991

3.3. Adsorption kinetics for single and binary dye solutions

It is important to be able to predict the rate at which contamination is removed from aqueous solutions in order to design an adsorption treatment plant. The mechanism of solute adsorption onto an adsorbent was studied by kinetic models. Several models were used. In order to design a fast and effective model, investigations were made on adsorption rate. For examination, the controlling mechanisms of adsorption process such as chemical reaction, diffusion control, and mass transfer several kinetics models are used to test the experimental data [9,63].

Pseudo-first-order equation is generally represented as follows (Eq. (13)) [64]:

$$dq_t/dt = k_1(q_e - q_t) \quad (13)$$

where q_t and k_1 are the amount of dye adsorbed at time t (mg/g) and the equilibrium rate constant of pseudo-first-order kinetics (1/min), respectively.

After integration by applying conditions, $q_t = 0$ at $t = 0$ and $q_t = q_t$ at $t = t$, then Eq. (13) becomes rearranged as Eq. (14) for single and Eq. (15) for binary dye solutions [65]:

$$\ln(q_e - q_t) = \ln(q_e) - k_1 t \quad (14)$$

$$\ln\left(\sum q_{e,i} - \sum q_{t,i}\right) = \ln\left(\sum q_{e,i}\right) - k_1 t \quad (15)$$

The straight-line plots of ln $(q_e - q_t)$ vs. t for single and binary dye solutions onto CNT at different dye concentrations have also been tested to obtain the rate parameters. The k_1, q_e, and correlation coefficients under different dye concentrations were calculated from these plots and are given in Table 4. This result indicated that the experimental data did not agree with the pseudo-first-order kinetic model.

Data were applied to the pseudo-second-order kinetic rate equation which is expressed as Eq. (16) [65]:

$$dq_t/dt = k_2(q_e - q_t)^2 \quad (16)$$

where k_2 is the equilibrium rate constant of pseudo-second-order (g/mg min). On integrating the Eq. (16), for single and binary dye mixtures, Eqs. (17) and (18) derived, respectively [65]:

$$t/q_t = 1/k_2 q_e{}^2 + t/q_e \quad (17)$$

$$t/\sum q_{t,i} = 1/k_2 \sum q_{e,i}{}^2 + t/\sum q_{e,i} \quad (18)$$

To understand the applicability of the model, linearized and non-linearized plots of t/q_t vs. time for the adsorption of dyes in single and binary systems onto CNT are plotted (Fig. 6). The k_2, q_e, and correlation

Table 4
Kinetic constants for dye adsorption on CNT at different dye concentrations for single and binary dye systems

	Pseudo-first-order			Pseudo-second-order		
Dye concentration	$q_{e,1}$	k_1	R^2	$q_{e,2}$	k_2	R^2
BB41						
25	14.983	0.091	0.831	76.923	0.029	1.000
50	71.154	0.104	0.876	120.482	0.005	0.997
75	67.593	0.067	0.911	140.845	0.004	0.996
100	80.798	0.061	0.877	161.290	0.003	0.995
BR18						
25	32.456	0.077	0.944	71.429	0.008	0.999
50	35.694	0.063	0.896	90.909	0.007	0.998
75	36.872	0.058	0.840	104.167	0.007	0.999
100	46.925	0.099	0.946	111.111	0.007	0.999
BV16						
25	25.445	0.065	0.911	56.818	0.009	0.998
50	29.648	0.046	0.815	74.074	0.007	0.997
75	30.088	0.057	0.805	81.967	0.008	0.998
100	28.477	0.049	0.803	83.333	0.008	0.998
BB41+BR18						
25	26.656	0.075	0.913	74.627	0.612	1.000
50	43.502	0.049	0.854	108.696	0.382	0.997
75	63.631	0.058	0.908	144.928	0.367	0.998
100	69.965	0.085	0.953	153.846	0.471	1.000
BB41+BV16						
25	27.635	0.039	0.744	72.464	0.548	0.999
50	37.728	0.049	0.798	107.527	0.596	0.999
75	50.084	0.062	0.864	129.870	0.484	1.000
100	56.031	0.057	0.867	147.059	0.475	0.999
BR18+BV16						
25	27.799	0.067	0.900	71.428	0.517	0.999
50	32.121	0.086	0.891	101.010	0.846	1.000
75	54.185	0.105	0.870	126.582	0.627	1.000
100	52.008	0.054	0.854	138.889	0.470	0.999

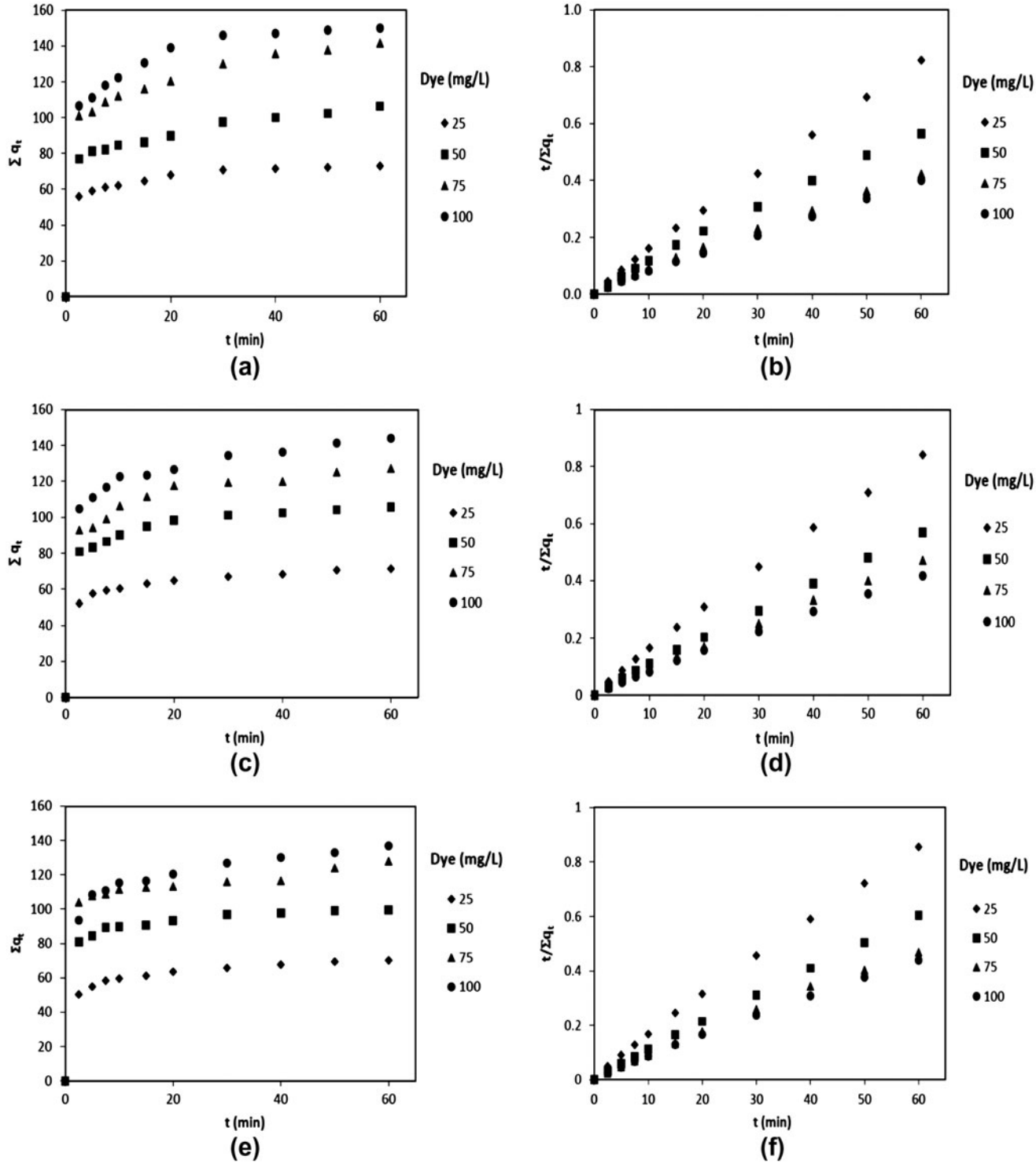

Fig. 6. Pseudo-second-order adsorption kinetic plot at different dye concentrations in binary system, (a) BB41 + BR18 (non-linearized), (b) BB41 + BR18 (linearized), (c) BB41 + BV16 (non-linearized), (d) BB41 + BV16 (linearized), (e) BR18 + BV16 (non-linearized), (f) BR18 + BV16 (linearized).

coefficients (R^2) were calculated from these plots and are given in Table 4.

The linearized and linearized fit between the t/q_t vs. contact time (t) and calculated R^2 for this kinetic model show that pseudo-second-order model with a good correlation coefficient ($R^2 = 0.99$) is more reliable model for this experiment at single and binary systems (Table 4 and Fig. 6). From Table 4, it is clear that the values of k_2 in binary systems were greater than those in single dye systems due to larger total initial dye concentration. In addition, the values of $q_{e,2}$ obtained from the regression calculation were relatively larger than the experimental values of $q_{e,1}$ [65].

3.4. Surface characteristics

In order to investigate the surface characteristics of CNT, FTIR is expressed in transmittance in 4,000–450 cm^{-1} range. Fig. 7 shows FTIR spectrum of CNT. The peak positions are at 3,437, 2,923, 2,858, 1,631, and 1,023 cm^{-1}. A broad absorption band around 3,400 cm^{-1} is attributed to the stretching vibration of the O–H while less intensive band at 1,631 cm^{-1} assigned to aromatic C=C groups which indicate graphite structure of multi-walled CNTs. The bands at 2,923 and 2,858 cm^{-1} correspond to asymmetric and symmetric aliphatic C–H stretching, respectively. Bands at 1,300–1,000 cm^{-1} correspond to C–O stretching which suggests the surface of CNT possesses some oxygen containing functional groups, thus providing a hydrophilic nature for CNT [66]. In addition FTIR spectra of dye adsorbed CNT were given. In case of dye adsorbed CNT additional peaks in the range of 1,100–1,350 cm^{-1} were observed which indicate C–N stretching groups due to the adsorption of basic dyes on the CNT surface. Moreover, the prominent peaks intensity are lower than that of raw CNT; this finding is apparently due to the fact that more functional groups such as O–H, C–O, and C=C are attached to the surface of the CNT. By comparing the FTIR of dye adsorbed CNT with raw CNT some shifting and extra peaks are observed which shows the adsorption of dyes on the surface of CNT [66,67].

To determine the zero point charge of CNT, 0.2 g of adsorbent was added to 40 mL of sodium nitrate at different pH values (pH = 2, 3, 4, 5, 6, 7, 8, 9, 10, and 11). Then the solutions were agitated at room temperature and their final pH values were measured [67]. Fig. 8 shows the final pH of the solutions against the initial pH. The pH_{zpc} for CNT is 6. At $pH > pH_{zpc}$ the surface of CNT has negatively charged favoring the adsorption of cationic species. Because the electrostatic interactions were the main adsorption mechanism, the basic dyes would have greater affinity to CNT surfaces at $pH > pH_{zpc}$. There are five main interactions for adsorption of an organic material on CNT including hydrophobic effect, π–π bonds, and hydrogen bonds, covalent and electrostatic interactions [68]. To explain the adsorption of organic materials on CNT two parallel adsorption mechanisms were reported including electrostatic and hydrophobic interactions [6,69]. Due to the acidic functional groups on the surface of the CNT, the net surface charge is negative. Hence, the electrostatic interactions between these

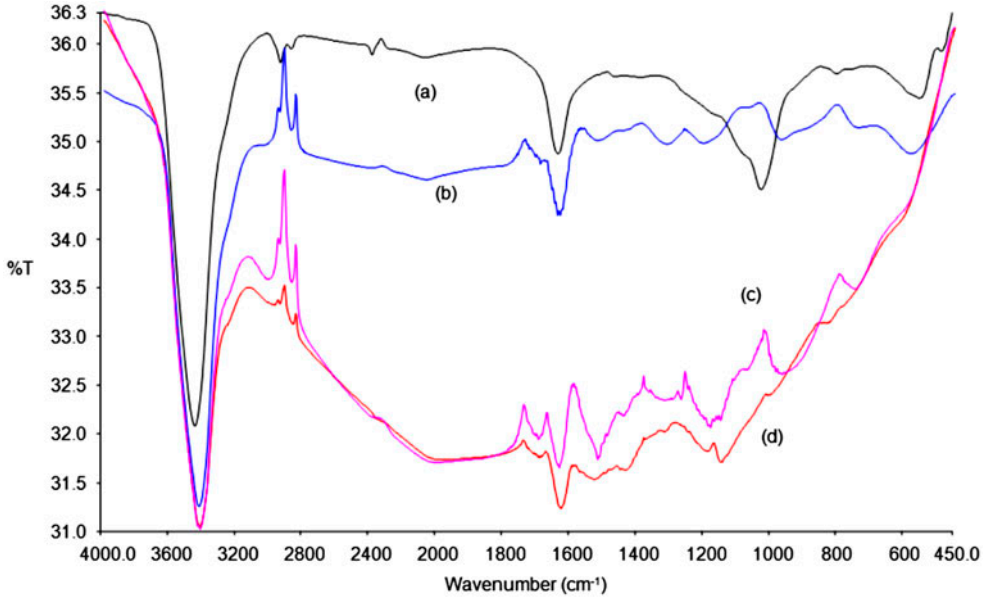

Fig. 7. FTIR spectrum (a) CNT, (b) BB41 adsorbed CNT, (c) BV16 adsorbed CNT, and (d) BR18 adsorbed CNT.

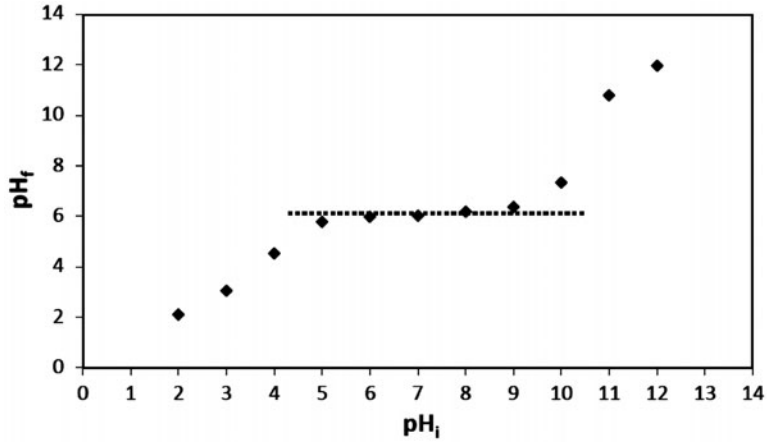

Fig. 8. Zero point charge of CNT.

negatively charged groups and positively charged dye molecules is the main factor for adsorption of basic dyes on the CNT surface. Moreover, because of the large surface area of CNT, the hydrophobic interactions can also be considered as a secondary factor which can has a synergy effect on the adsorption process.

4. Conclusion

In this manuscript, the ability of multi-walled CNT to adsorb three cationic dyes from colored wastewater in single and binary systems was studied. BB41, BR18, and BV16 were used as model dyes. CNT exhibited high sorption capacity toward basic dyes. The equilibrium data were correlated reasonably well by Langmuir and extended Langmuir adsorption isotherm models. The single system isotherm for BB41, BR18, and BV16 has the monolayer saturation capacities of 123.5, 80.0, and 63.9 mg/g, respectively. The adsorption isotherm of an individual dye in binary dye solutions followed an extended Langmuir isotherm model. The adsorption kinetics for the three dyes from single dye systems, and the total amounts of dyes adsorbed from binary dye solutions, followed the pseudo-second-order kinetic model. The adsorption rate constants were observed to increase with increasing CNT dosage. Results showed that CNT can be used effectively as an adsorbent for the removal of cationic dyes from single and binary systems.

References

[1] N.M. Mahmoodi, Photocatalytic ozonation of dyes using multiwalled carbon nanotube, J. Mol. Catal. A: Chem. 366 (2013) 254–260.

[2] N.M. Mahmoodi, Magnetic ferrite nanoparticle–alginate composite: Synthesis, characterization and binary system dye removal, J. Taiwan Inst. Chem. Eng. 44 (2013) 321–329.

[3] N.M. Mahmoodi, Synthesis of amine-functionalized magnetic ferrite nanoparticle and its dye removal ability, J. Environ. Eng. 139 (2013) 1382–1390.

[4] N.M. Mahmoodi, Photodegradation of dyes using multiwalled carbon nanotube and ferrous ion, J. Environ. Eng. 139 (2013) 1368–1374.

[5] S. Wang, C.W. Ng, W. Wang, Q. Li, L. Li, A comparative study on the adsorption of acid and reactive dyes on multiwall carbon nanotubes in single and binary dye systems, J. Chem. Eng. Data 57 (2012) 1563–1569.

[6] S. Wang, C.W. Ng, W. Wang, Q. Li, Z. Hao, Synergistic and competitive adsorption of organic dyes on multiwalled carbon nanotubes, Chem. Eng. J. 197 (2012) 34–40.

[7] Y. Bulut, H. Aydin, A kinetics and thermodynamics study of methylene blue adsorption on wheat shells, Desalination 194 (2006) 259–267.

[8] N.K. Amin, Removal of reactive dye from aqueous solutions by adsorption onto activated carbons prepared from sugarcane bagasse pith, Desalination 223 (2008) 152–161.

[9] G. Crini, P.M. Badot, Application of chitosan, a natural aminopolysaccharide, for dye removal from aqueous solutions by adsorption processes using batch studies: A review of recent literature, Prog. Polym. Sci. 33 (2008) 399–447.

[10] M. Uğurlu, Adsorption of a textile dye onto activated sepiolite, Microporous Mesoporous Mater. 119 (2009) 276–283.

[11] V.K. Gupta, R. Jain, S. Varshney, Removal of Reactofix golden yellow 3 RFN from aqueous solution using wheat husk—An agricultural waste, J. Hazard. Mater. 142 (2007) 443–448.

[12] A. Mittal, V.K. Gupta, A. Malviya, J. Mittal, Process development for the batch and bulk removal and recovery of a hazardous, water-soluble azo dye (Metanil Yellow) by adsorption over waste materials (Bottom Ash and De-Oiled Soya), J. Hazard. Mater. 151 (2008) 821–832.

[13] D. Mohan, K.P. Singh, S. Sinha, D. Gosh, Removal of pyridine derivatives from aqueous solution by activated carbons developed from agricultural waste materials, Carbon 43 (2005) 1680–1693.
[14] V.K. Gupta, B. Gupta, A. Rastogi, S. Agarwal, A. Nayak, A comparative investigation on adsorption performances of mesoporous activated carbon prepared from waste rubber tire and activated carbon for a hazardous azo dye—Acid Blue 113, J. Hazard. Mater. 186 (2011) 891–901.
[15] A.K. Jain, V.K. Gupta, A. Bhatnagar, Suhas, A comparative study of adsorbents prepared from industrial wastes for removal of dyes, Sep. Sci. Technol. 38 (2003) 463–481.
[16] V.K. Gupta, S. Sharma, Removal of zinc from aqueous solutions using bagasse fly ash—A low cost adsorbent, Ind. Eng. Chem. Res. 42 (2003) 6619–6624.
[17] S. Karthikeyan, V.K. Gupta, R. Boopathy, A. Titus, G. Sekaran, A new approach for the degradation of high concentration of aromatic amine by heterocatalytic Fenton oxidation: Kinetic and spectroscopic studies, J. Mol. Liq. 173 (2012) 153–163.
[18] V.K. Gupta, R. Jain, S. Varshney, Electrochemical removal of the hazardous dye Reactofix Red 3 BFN from industrial effluents, J. Colloid Interface Sci. 312 (2007) 292–296.
[19] V.K. Gupta, R. Jain, A. Mittal, M. Mathur, S. Sikarwar, Photochemical degradation of the hazardous dye Safranin-T using TiO_2 catalyst, J. Colloid Interface Sci. 309 (2007) 464–469.
[20] V.K. Gupta, I. Ali, T.A. Saleh, A. Nayak, S. Agarwal, Chemical treatment technologies for waste-water recycling—an overview, RSC Adv. 2 (2012) 6380–6388.
[21] V.K. Gupta, A. Rastogi, A. Nayak, Biosorption of nickel onto treated alga (*Oedogonium hatei*): Application of isotherm and kinetic models, J. Colloid Interface Sci. 342 (2010) 533–539.
[22] V.K. Gupta, I. Ali, V.K. Saini, Defluoridation of wastewaters using waste carbon slurry, Water Res. 41 (2007) 3307–3316.
[23] A. Jain, V. Gupta, S. Jain, Removal of chlorophenols using industrial wastes, Environ. Sci. Technol. 38 (2004) 1195–1200.
[24] N.K. Amin, Removal of direct blue-106 dye from aqueous solution using new activated carbons developed from pomegranate peel: Adsorption equilibrium and kinetics, J. Hazard. Mater. 165 (2009) 52–62.
[25] V.K. Gupta, A. Mittal, L. Kurup, J. Mittal, Adsorption of a hazardous dye, erythrosine, over hen feathers, J. Colloid Interface Sci. 304 (2006) 52–57.
[26] V.K. Gupta, A. Mittal, A. Malviya, J. Mittal, Adsorption of carmoisine A from wastewater using waste materials—Bottom ash and deoiled soya, J. Colloid Interface Sci. 335 (2009) 24–33.
[27] V.K. Gupta, S. Sharma, Removal of zinc from aqueous solutions using bagasse fly ash − A low cost adsorbent, Ind. Eng. Chem. Res. 42 (2003) 6619–6624.
[28] C. Lu, Y.L. Chung, K.F. Chang, Adsorption of trihalomethanes from water with carbon nanotubes, Water Res. 39 (2005) 1183–1189.
[29] H. Yan, A. Gong, H. He, J. Zhou, Y. Wei, L. Lv, Adsorption of microcystins by carbon nanotubes, Chemosphere 62 (2006) 142–148.
[30] Y.H. Li, S. Wang, A. Cao, D. Zhao, X. Zhang, C. Xu, Z. Luan, D. Ruan, J. Liang, D. Wu, B. Wei, Adsorption of fluoride from water by amorphous alumina supported on carbon nanotubes, Chem. Phys. Lett. 350 (2001) 412–416.
[31] Y.H. Li, S. Wang, J. Wei, X. Zhang, C. Xu, Z. Luan, D. Wu, B. Wei, Lead adsorption on carbon nanotubes, Chem. Phys. Lett. 357 (2002) 263–266.
[32] C. Chen, X. Wang, Adsorption of Ni(II) from aqueous solution using oxidized multiwall carbon nanotubes, Ind. Eng. Chem. Res. 45 (2006) 9144–9149.
[33] X. Peng, Z. Luan, J. Ding, Z. Di, Y. Li, B. Tian, Ceria nanoparticles supported on carbon nanotubes for the removal of arsenate from water, Mater. Lett. 59 (2005) 399–403.
[34] S. Iijima, Helical microtubules of graphitic carbon, Nature 354 (1991) 56–58.
[35] N. Jha, S. Ramaprabhu, Thermal conductivity studies of metal dispersed multiwalled carbon nanotubes in water and ethylene glycol based nanofluids, J. Appl. Phys. 106 (2009) 84317–84326.
[36] D.H. Lin, B.S. Xing, Adsorption of phenolic compounds by carbon nanotubes: Role of aromaticity and substitution of hydroxyl groups, Environ. Sci. Technol. 42 (2008) 7254–7259.
[37] B. Pan, B. Xing, Adsorption mechanisms of organic chemicals on carbon nanotubes, Environ. Sci. Technol. 42 (2008) 9005–9013.
[38] T.A. Saleh, V.K. Gupta, Column with CNT/magnesium oxide composite for lead(II) removal from water, Environ. Sci. Pollut. Res. 19 (2012) 1224–1228.
[39] V.K. Gupta, S. Agarwal, T.A. Saleh, Chromium removal by combining the magnetic properties of iron oxide with adsorption properties of carbon nanotubes, Water Res. 45 (2011) 2207–2212.
[40] J.L. Gong, B. Wang, G.M. Zeng, C.P. Yang, C.G. Niu, Q.Y. Niu, W.J. Zhou, Y. Liang, Removal of cationic dyes from aqueous solution using magnetic multi-wall carbon nanotube nanocomposite as adsorbent, J. Hazard. Mater. 164 (2009) 1517–1522.
[41] H.B. Li, X.C. Gui, L.H. Zhang, S.S. Wang, C.Y. Ji, J.Q. Wei, K.L. Wang, H.W. Zhu, D.H. Wu, A.Y. Cao, Carbon nanotube sponge filters for trapping nanoparticles and dye molecules from water, Chem. Commun. 46 (2010) 7966–7968.
[42] N.M. Mahmoodi, R. Salehi, M. Arami, Binary system dye removal from colored textile wastewater using activated carbon: Kinetic and isotherm studies, Desalination 272 (2011) 187–195.
[43] M. Yazdani, N.M. Mahmoodi, M. Arami, H. Bahrami, Surfactant-modified feldspar: Isotherm, kinetic, and thermodynamic of binary system dye removal, J. Appl. Polym. Sci. 126 (2012) 340–349.
[44] N.M. Mahmoodi, Equilibrium, kinetics, and thermodynamics of dye removal using alginate in binary systems, J. Chem. Eng. Data 56 (2011) 2802–2811.
[45] N.M. Mahmoodi, B. Hayati, M. Arami, F. Mazaheri, Single and binary system dye removal from colored textile wastewater by a dendrimer as a polymeric nanoarchitecture: Equilibrium and kinetics, J. Chem. Eng. Data 55 (2010) 4660–4668.
[46] K.K.H. Choy, J.F. Porter, G. McKay, Langmuir isotherm models applied to the multicomponent sorption

of acid dyes from effluent onto activated carbon, J. Chem. Eng. Data 45 (2000) 575–584.
[47] M.S. Chiou, H.Y. Li, Adsorption behavior of reactive dye in aqueous solution on chemical cross-linked chitosan beads, Chemosphere 50 (2003) 1095–1105.
[48] S. Chatterjee, S. Chatterjee, B.P. Chatterjee, A.R. Das, A.K. Guha, Adsorption of a model anionic dye, eosin Y, from aqueous solution by chitosan hydrobeads, J. Colloid Interface Sci. 288 (2005) 30–35.
[49] I. Langmuir, The constitution and fundamental properties of solids and liquids. Part I. Solids, J. Am. Chem. Soc. 38 (1916) 2221–2295.
[50] Y. Yao, F. Xu, M. Chen, Z. Xu, Z. Zhu, Adsorption behavior of methylene blue on carbon nanotubes, Bioresour. Technol. 101 (2010) 3040–3046.
[51] K. Yang, B. Xing, Adsorption of organic compounds by carbon nanomaterials in aqueous phase: Polanyi theory and its application, Chem. Rev. 110 (2010) 5989–6008.
[52] D.H. Lin, B.S. Xing, Adsorption of phenolic compounds by carbon nanotubes: Role of aromaticity and substitution of hydroxyl groups, Environ. Sci. Technol. 42 (2008) 7254–7259.
[53] G. McKay, J.F. Porter, G.R. Prasad, The removal of dye colours from aqueous solutions by adsorption on low-cost materials, Water Air Soil Pollut. 114 (1999) 423–438.
[54] M. Otero, F. Rozada, L.F. Calvo, A.I. García, A. Morán, Kinetic and equilibrium modelling of the methylene blue removal from solution by adsorbent materials produced from sewage sludges, Biochem. Eng. J. 15 (2003) 59–68.
[55] N. Kannan, M.M. Sundaram, Kinetics and mechanism of removal of methylene blue by adsorption on various carbons—A comparative study, Dyes Pigm. 51 (2001) 25–40.
[56] F. Banat, S. Al-Asheh, L. Al-Makhadmeh, Evaluation of the use of raw and activated date pits as potential adsorbents for dye containing waters, Process Biochem. 39 (2003) 193–202.
[57] M. Bagane, S. Guiza, Elimination d'un colorant des effluents de l'industrie textile par adsorption, Ann. Chim. Sci. Mat. 25 (2000) 615–625.
[58] M.A. Al-Ghouti, M.A. Khraisheh, S.J. Allen, M.N. Ahmad, The removal of dyes from textile wastewater: A study of the physical characteristics and adsorption mechanisms of diatomaceous earth, J. Environ. Manage. 69 (2003) 229–238.
[59] A.K. Jain, V.K. Gupta, A. Bhatnagar, S. Jain, A comparative assessment of adsorbents prepared from industrial wastes for the removal of cationic dye, J. Indian Chem. Soc. 80 (2003) 267–270.
[60] K.K.H. Choy, J.F. Porter, G. McKay, Langmuir isotherm models applied to the multicomponent sorption of acid dyes from effluent onto activated carbon, J. Chem. Eng. Data 45 (2000) 575–584.
[61] T. Sismanoglu, Y. Kismir, S. Karakus, Single and binary adsorption of reactive dyes from aqueous solutions onto clinoptilolite, J. Hazard. Mater. 184 (2010) 164–169.
[62] N.M. Mahmoodi, R. Salehi, M. Arami, H. Bahrami, Dye removal from colored textile wastewater using chitosan in binary systems, Desalination 267 (2011) 64–72.
[63] Y.S. Ho, Adsorption of heavy metals from waste streams by peat, PhD thesis, The University of Birmingham, Birmingham, 1995.
[64] S. Lagergren, Zur theorie der sogenannten adsorption gelöster stoffe, K. Sven. Vetenskapsakad. Handl. 24 (1898) 1–39.
[65] D. Shena, J. Fana, W. Zhoub, B. Gaob, Q. Yueb, Q. Kanga, Adsorption kinetics and isotherm of anionic dyes onto organo-bentonite from single and multisolute systems, J. Hazard. Mat. 172 (2009) 99–107.
[66] D.L. Pavia, G.M. Lampman, G.S. Kaiz, Introduction to spectroscopy: A guide for students of organic chemistry, W.B. Saunders, New York, NY, 1987.
[67] A.K. Mishra, T. Arockiadoss, S. Ramaprabhu, Study of removal of azo dye by functionalized multi walled carbon nanotubes, Chem. Eng. J. 162 (2010) 1026–1034.
[68] C.H. Wu, Adsorption of reactive dye onto carbon nanotubes: Equilibrium, kinetics and thermodynamics, J. Hazard. Mater. 144 (2007) 93–100.
[69] A. Mittal, J. Mittal, A. Malviya, D. Kaur, V.K. Gupta, Adsorption of hazardous dye crystal violet from wastewater by waste materials, J. Colloid Interface Sci. 343 (2010) 463–473.